INSTITUTE OF PHYSICS PUBLISHING NANOTECHNOLOGY
Nanotechnology **18** (2007) 084001 (10pp) doi:10.1088/0957-4484/18/8/084001

Japan AFM roadmap 2006

Seizo Morita[1], **Hirofumi Yamada**[2] **and Toshio Ando**[3]

[1] Department of Electrical, Electronic and Information Engineering, Graduate School of Engineering, Osaka University, Suita, Osaka 565-0871, Japan
[2] Department of Electronic Science and Engineering, Kyoto University, Katsura, Nishikyo, Kyoto 615-8510, Japan
[3] Department of Physics, Faculty of Science, Kanazawa University, Kakuma-machi, Kanazawa, 920-1192, Japan

Received 21 July 2006, in final form 25 October 2006
Published 18 January 2007
Online at stacks.iop.org/Nano/18/084001

Abstract
This article reviews recent progress in Japan in the techniques and applications of dynamic mode atomic force microscopy (AFM), specifically focusing on three topics: (1) mechanical discrimination of intermixed two-atom species and their manipulation by frequency modulation (FM) AFM under ultrahigh vacuum; (2) sub-molecular and atomic-resolution imaging in liquids by FM-AFM; and (3) high-speed imaging of biological macromolecules in solution by amplitude modulation (AM) AFM. After reviewing the state of the art of these high-performance AFMs and various techniques that have enabled them, we present future prospects for these AFMs and for technological innovations that will be led by them. These prospects are given from the viewpoint of Japanese groups that have been involved in these three topics.

1. Introduction

In 1986, the atomic force microscope (AFM) was invented as a novel atomic-resolution microscope [1], which was capable of imaging even insulating surfaces, unlike the scanning tunnelling microscope. In the early stages, however, static contact AFM could not achieve stable and reproducible atomic resolution because of the destruction of the surface and tip apex due to a strong interaction force between them. In order to reduce this interaction force, dynamic mode AFM [2], including non-contact AFM [3], was devised, wherein the cantilever is oscillated. At present, using dynamic mode AFM, true atomic-resolution imaging under ultrahigh vacuum (UHV) [4] is routinely carried out.

Various technological developments and applied studies have continued using dynamic mode AFM, and this progress is expected to continue further. It seems worthwhile to consider, at the current stage, its prospects for potential developments and directions to go forward. From a wide range of studies using dynamic mode AFM, here we consider three recent topics in which the authors (three different Japanese groups) have been actively involved: chemical identification of single atoms [5] and selected-atom manipulation [6] in UHV; high-resolution imaging in a liquid [7]; and high-speed imaging in a liquid [8]. These three lines of investigation have become important issues in AFM and are currently being actively studied. In the present article, we review the techniques that have made these studies possible, briefly introduce some studies that are currently underway for further progress, and then present roadmaps for these three topics from our point of view. Roadmaps for a vast range of scanning probe microscopy are given by [9].

2. Atomic discrimination, manipulation, and assembly

The frequency modulation (FM) detection method, combined with the large oscillation amplitude of the cantilever [2], has enabled the achievement of true atomic resolution using dynamic mode AFM in UHV [3, 4] (UHV-FM-AFM). To expand the ability of UHV-FM-AFM at room temperature (RT) further toward atomic discrimination, manipulation and assembly, the stabilities of both the imaging area and the tip–sample distance are crucial issues. In the case of conventional UHV-FM-AFM, the typical value of thermal drift over the imaging area is nearly 10 Å min^{-1}, which would disturb the positioning for atom discrimination, manipulation and assembly. In the case of our home-built UHV-FM-AFM, however, thermal drift is typically 3 Å min^{-1} even at RT, and sometimes close to 1 Å min^{-1}. Furthermore, we used an atom-tracking technique to compensate for thermal drift, in addition to using our home-built UHV-FM-AFM with low thermal drift.

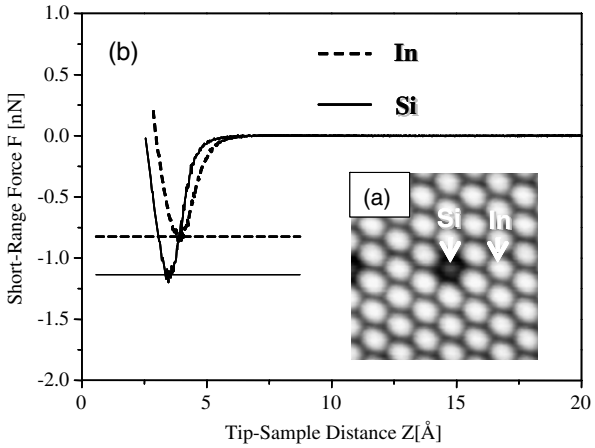

Figure 1. Chemical discrimination of In and Si adatoms on a In/Si(111)$\sqrt{3}\times\sqrt{3}$ pure phase (In 1/3 ML) surface using (a) non-contact AFM topography (inset image: 4.2 nm × 4.2 nm), and (b) short-range force curves of selected In and Si atoms indicated by the white arrows in (a) at RT.

It was shown that the precision of positioning control at RT is better than 0.2 Å peak-to-peak [10], with lateral stability comparable to that in cryogenic inelastic electron tunnelling spectroscopy measurements [11].

2.1. Topography-based atom discrimination

UHV-FM-AFM under attractive force was able to achieve chemical discrimination of atom species using topography-based atom-selective imaging based on the atomic force of individual atoms [5]. The inset in figure 1 shows non-contact AFM topography of In/Si(111) $\sqrt{3}\times\sqrt{3}$ pure phase (In 1/3 monolayer, ML) at RT. We can clearly observe a few small, dim substituted Si adatoms. Thus, this AFM topography image shows chemical contrast by atom-selective imaging between the In and Si adatoms. Such chemical contrast utilizes the height difference in the topographic image, and hence requires an atomically flat surface for chemical discrimination of atom species. Recently, we succeeded in measuring precise frequency shift as a function of tip–sample distance (frequency shift curve) of selected atoms even at RT [5] by compensating for thermal drift using the atom-tracking technique and by averaging many frequency shift curves of selected atoms [10]. By converting a site-specific frequency shift curve to a site-specific force curve and simultaneously subtracting the long-range force contribution due to the van der Waals force [5], we have obtained precise short-range force curves of selected In and Si adatoms, indicated by the white arrows in the inset in figure 1(a). From figure 1(b), it was confirmed that the Si atom has a larger covalent bonding force than the In atom. Therefore, in principle, such short-range force curves of selected atoms enable us to discriminate between chemical species of individual atoms. This method thus is topography-based atom discrimination, since it needs a topographic image of the surface with atomic resolution for choosing the target atom. The advantage of this method is that it enables us to clarify the chemical covalent force over each species independently of the tip–surface distance.

2.2. Roadmap towards chemical identification of atom species

Figure 2 shows a roadmap (status and future prospects) towards chemical identification of atom species by AFM. The results achieved thus far include chemical discrimination of periodic lattice atoms, such as In and As atoms in InAs(110) [12], and Ca and F atoms in CaF_2(111) [13], and that of intermixed aperiodic atoms such as Cl and Br atoms in $KCl_{0.6}Br_{0.4}$(100) [14], Si and Sb atoms in Si(111)5$\sqrt{3}\times$

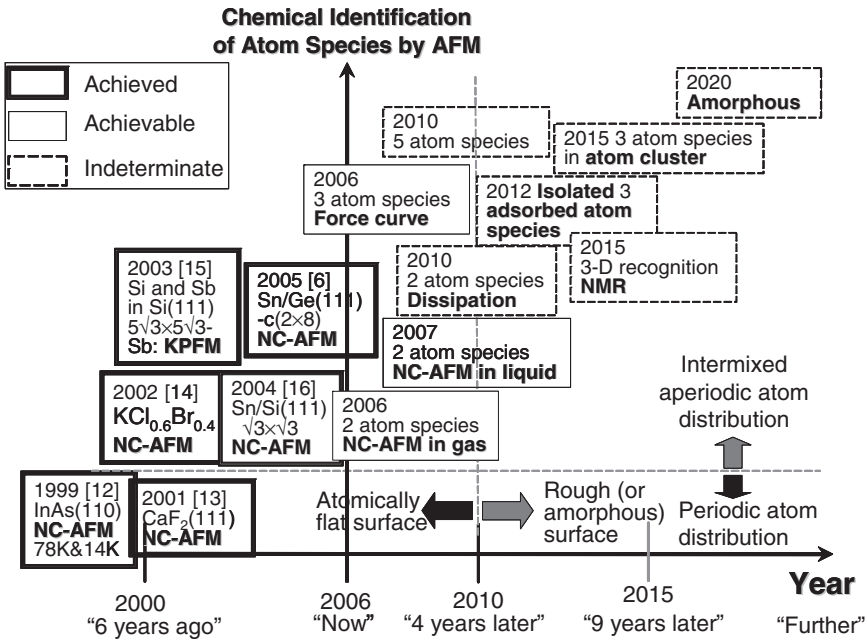

Figure 2. Roadmap toward chemical identification of atom species by AFM.

$5\sqrt{3}$-Sb [15], Sn and Si atoms in Sn/Si(111)$\sqrt{3} \times \sqrt{3}$ [16], and Sn and Ge atoms in Sn/Ge(111)-c(2 × 8) [6]. NC-AFM, KPFM and the force curve represent non-contact AFM topography, Kelvin probe force microscopy and site-specific force curve, respectively. Thus, chemical discrimination of atom species has developed from easier systems with periodic atoms to more difficult ones with intermixed aperiodic atoms. The mainstream until 2010 related to chemical identification of atom species will be the achievement of chemical discrimination using other methods such as force curve and energy dissipation, and the realization of chemical discrimination in non-UHV environments such as a gas or a liquid. Chemical discrimination of insulator and metallic atoms will also become important subjects to widen the range of applicable materials. After 2010, the target of chemical identification will move from easier samples with atomically flat surfaces to more difficult ones with rough surfaces, such as isolated adsorbed atoms and atom clusters for the assembly of complex compound nanostructures. Chemical contrast in non-contact AFM topography, however, utilizes height differences in the topographic image and hence requires an atomically flat surface. Therefore, we cannot use this method for a rough (or corrugated) sample surface such as a three-dimensional atom cluster. On the other hand, short-range force curves of single atoms can discriminate between atom species using not the height difference but the force difference, so that we can use this method even for rough (or corrugated) sample surfaces. However, short-range force curves of single atoms as well as non-contact AFM topography use the atomic force. Therefore, chemical discrimination of individual atoms on an amorphous surface, whose atomic force will have a wide variation due to the amorphous structure, appears to be a very difficult and challenging subject. Further, true chemical identification, that is, universal chemical identification of unknown single atoms is the most important issue. Not only true chemical identification but also three-dimensional recognition (tomography) may be achievable using a nuclear magnetic resonance (NMR) technique such as magnetic resonance force spectroscopy (MRFM) [17].

2.3. Atom manipulation and assembly from multi-atom species

UHV-FM-AFM was used to achieve not only vertical atom manipulation, such as atom extraction and atom deposition [18], but also lateral atom manipulation [19] of selected individual atoms by precisely controlling the lateral and vertical tip position around the near-contact region [19] at low temperature (LT). Recently, we found a lateral atom-interchange manipulation phenomenon between a substituted Sn adatom and an adjacent Ge adatom on a Sn/Ge(111)-c(2 × 8) surface at RT [6]. Using the vector scan, we succeeded in directional atom interchange between a selected Sn adatom and a selected adjacent Ge adatom. We were then able to construct embedded atom letters or an atom inlay, by forming 'Sn' (the symbol for a tin atom) on the surface consisting of 19 slightly larger Sn atoms embedded in the smaller Ge atoms of a Ge(111) substrate, as shown in figure 3. To construct the atom inlay shown in figure 3, we needed 9 h and 120 times the lateral atom interchange between Sn and Ge adatoms. It should be remarked that not only the minimum force for atom interchange but also the appearance of such a phenomenon itself depends on the tip.

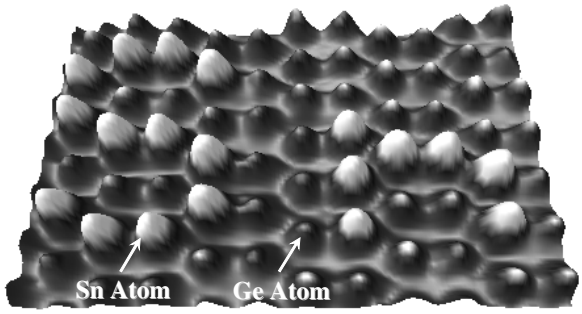

Figure 3. Protruded 'atom inlay', that is, the atom letters 'Sn' consisting of a slightly large 19 Sn adatoms embedded in a little small Ge adatoms on Sn/Ge(111)-c(2 × 8) surface at RT.

2.4. Roadmap for mechanical atom manipulation and assembly

Figure 4 shows a roadmap for mechanical atom manipulation and assembly by AFM. Results achieved thus far include conventional vertical [3, 18] and lateral [18] atom manipulations in UHV at LT that moved only one kind of atom species, and lateral atom-interchange manipulation at RT that moved heterogeneous two-atom species by tip-induced directional atom interchange. Thus, mechanical atom manipulation by AFM was developed from simpler manipulation of single-atom species to more complex manipulation of multi-atom species. Very recently, atomistic manipulations on insulating surfaces were achieved [20, 21]. A manipulated atomic-scale object, however, seems to be an atomic-scale defect or adsorbed molecule. Further, site-by-site positioning by atom manipulation is still incomplete. In 2006, site-by-site manipulation of a single atom selected from multi atom species on insulating surface may be achievable. By 2010, chemical identification of intermixed heterogeneous atoms on an insulating surface and following selected atom manipulation will become important subjects in UHV. Besides, the manipulation of single atoms in a gas and liquid will also become an important subject. After 2010, the assembly of atom clusters and atom devices with novel functions from multi-atom species at RT will become important. Selected atom manipulation of intermixed multi-atom species and artificial nanostructuring in gases and liquids will also become important. Furthermore, the development of a technique that can arbitrarily construct designed molecules from individual atoms using observation, chemical identification and manipulation of atoms is the most difficult and challenging issue for atom manipulation. Such a technology may enable us to construct complex molecules and high polymers from multi-atom species in the future. The assembly of molecules using two-atom species is the first step in this direction.

3. Atomic resolution in a liquid

Atomic-scale FM-AFM imaging of atomically flat samples in UHV environments is now becoming routine. High-resolution imaging in a liquid has been greatly anticipated, especially for

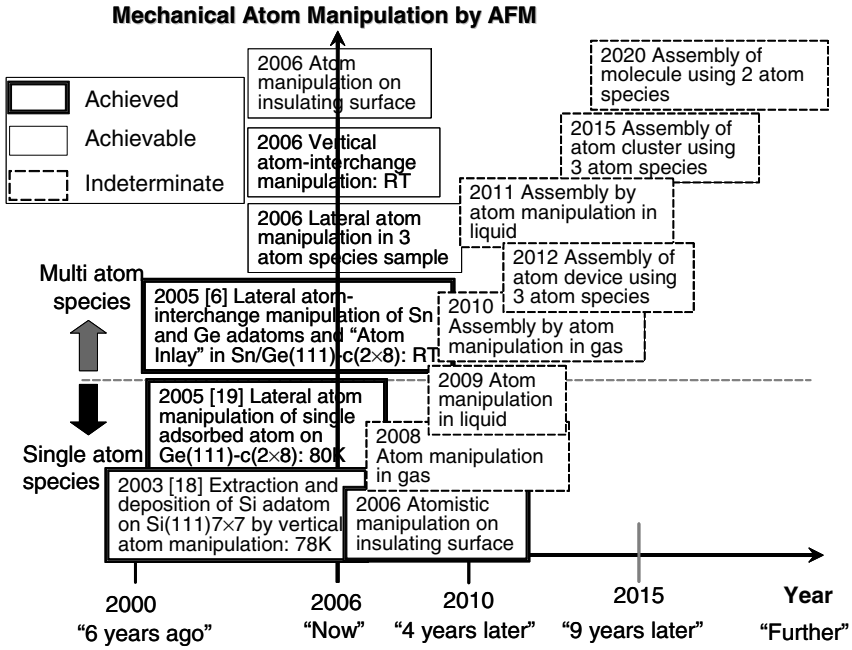

Figure 4. Roadmap for mechanical atom manipulation by AFM.

biological studies. However, the imaging capability in liquids by FM-AFM is severely hindered by the extreme reduction of the cantilever Q-factor due to hydrodynamic interaction between the cantilever and the liquid. The Q-factors in UHV usually exceed 10 000, while those in liquid environments are smaller than 10. In fact, it was not certain that FM-AFM would work in such an environment with a low Q-factor, because a high Q-factor of the cantilever is indispensable for stable operation of an FM-AFM with an electromechanical resonator for its self-oscillation circuit.

The use of the small-amplitude mode and large noise reduction in the cantilever deflection sensor have resulted in great progress in FM-AFM imaging in liquids [7, 22, 23]. Short-range chemical interactions between a tip and a sample surface occur only when the tip is in close proximity to the surface. Thus, the force sensitivity can be increased by FM detection with small-amplitude oscillation because of the increase in the effective duration of the proximity interactions. Note that the small-amplitude mode can only be used when the noise in the deflection sensor (usually in the laser beam deflection method) is sufficiently reduced to the level of thermal fluctuations in the cantilever. On the other hand, we have to consider the increase in the phase noise of the FM detector caused by a decrease in the oscillation amplitude, since the noise is proportional to the reciprocal of the amplitude.

3.1. Development of low-noise FM-AFM

The shot noise in the laser beam deflection sensor, as shown in figure 5, gives the theoretical limit of the minimum noise for signal detection. Apart from the shot noise, other dominant noises in the sensor are the 'optical feedback noise' and 'optical interference noise', both of which originate in the high coherence of the laser light. The modulation of laser power with a high-frequency (HF) signal whose frequency was typically 300–500 MHz was effective in reducing the coherence and hence the noise [24]. We applied this technique to the deflection sensor as shown in figure 5. Figure 6 shows the frequency spectra of cantilever Brownian motion measured using the improved deflection sensor in water. The solid line shows an experimentally measured curve using the improved deflection sensor, while the dotted curve shows a theoretical curve calculated using the following equation for the displacement noise density $N_{\mathrm{th}}(f)$:

$$N_{\mathrm{th}}(f) = \sqrt{\frac{1}{\left[1-(f/f_0)^2\right]^2 + \left[f/(f_0 Q)\right]^2}\frac{2k_{\mathrm{B}}T}{\pi f_0 k Q}} \qquad (1)$$

where f, f_0, k, k_{B} and T are the vibration frequency, resonance frequency, spring constant of a cantilever, Boltzmann constant and temperature, respectively.

The peaks observed in the spectra correspond to the Brownian vibration at the cantilever resonance, while the background white noise (grey horizontal line in figure 6) comes from the deflection sensor noise. The results reveal that the deflection noise densities arising from our deflection sensor were 17 fm $\mathrm{Hz}^{-\frac{1}{2}}$ in air and 39 fm $\mathrm{Hz}^{-\frac{1}{2}}$ in liquid. These values are much smaller than the deflection noise densities obtained with a deflection sensor in commercially available AFMs (typically 100–1000 fm $\mathrm{Hz}^{-\frac{1}{2}}$ in air). Since the bandwidth of the FM detector (B_{FM}) is usually less than 1 kHz, the deflection noise components, which induce frequency noises, should be in the frequency range from f_0 to $f_0 + 1$ kHz. In this frequency regime, the experimentally measured values are nearly the same as the theoretically calculated values in both air and liquid environments.

Consequently, true atomic-resolution imaging in a liquid was successfully achieved by FM-AFM [7, 22]. Figure 7 shows an FM-AFM image of a cleaved (001) surface of muscovite

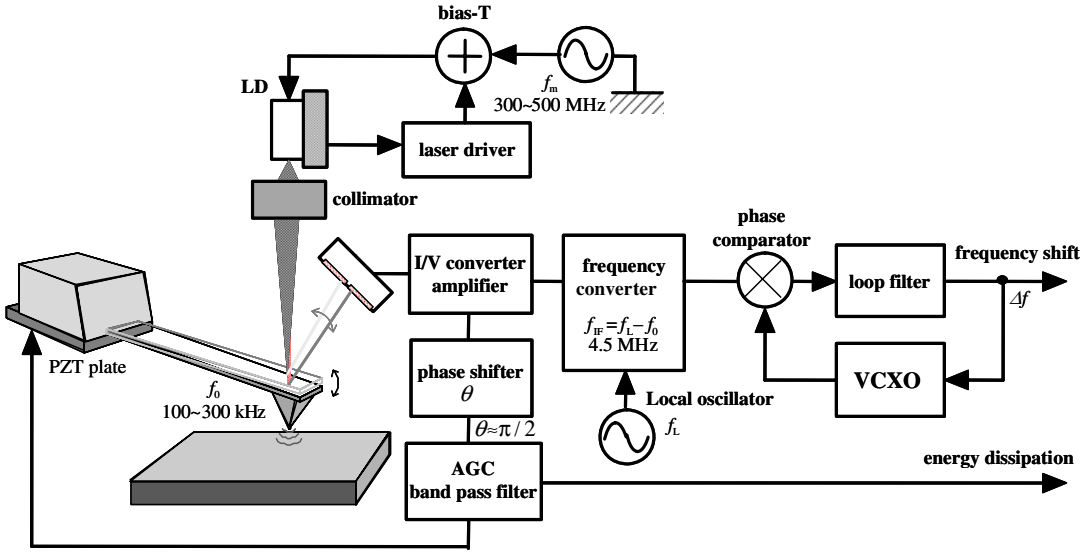

Figure 5. Schematic of an experimental setup in FM-AFM.

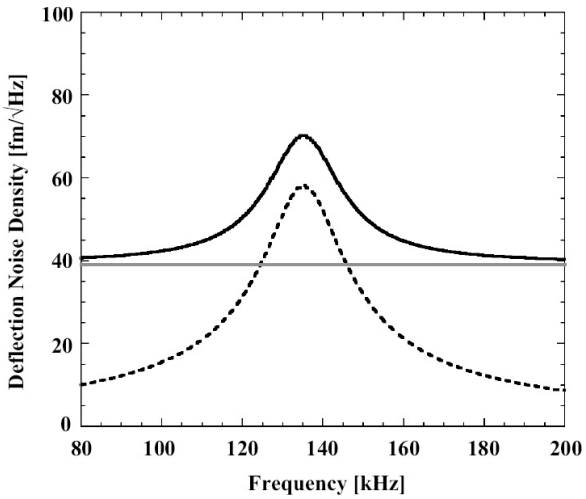

Figure 6. Frequency spectra of cantilever Brownian motion. Solid curve: spectrum measured using the improved deflection sensor in water ($k = 40$ N m^{-1}, $Q = 8$). Dotted curve: theoretical spectrum curve calculated using equation (1). Grey horizontal line: estimated sensor noise level (39 fm Hz$^{-\frac{1}{2}}$).

mica obtained in pure water. Atomic-scale features with a period of 0.52 nm are clearly imaged. These features were stably obtained with frequency shifts in the range from +200 to +500 Hz. The vertical resolution of the FM-AFM was calculated from the measured frequency shift curve and the frequency noise with an FM bandwidth of 1 kHz. The obtained value of the vertical resolution was 2–6 pm. Since the vertical corrugation of the atomic surface is typically 20–100 pm, a vertical resolution of 2–6 pm is sufficiently small to achieve true atomic resolution. Figure 8 shows an FM-AFM image of a purple membrane containing bacteriorhodopsin (bR) protein molecules on a mica substrate in a phosphate buffer solution. We can clearly see the regular hexagonal arrangement of sets of three bright dots corresponding to bR trimers, as well as some defects in the trimers (indicated by the white arrows).

3.2. Roadmap of FM-AFM imaging in liquids

AFM imaging in liquids has been applied to studies of biological samples for a long time, since the early stages of its development. There has been tremendous and rapid progress in AFM imaging techniques in liquids such as the Q-control method and high-resolution imaging using FM-AFM. Figure 9 shows a technology roadmap for AFM measurements in a liquid, based on possible technological developments as well as user demand. For practical imaging applications, the imaging of a sample with a large height difference in topography is unavoidable. However, in FM-AFM imaging of such a sample, the cantilever oscillation tends to be unstable or stops, in the worst case. When the oscillation stops, the AFM imaging signal is inevitably lost; in addition, the tip can crash anytime into the sample. By setting the frequency shift to a small value (the tip is positioned far from the sample surface), the risk of stopping of the oscillation can be eliminated at the severe sacrifice of imaging resolution. A new intelligent control method for the frequency shift, which changes flexibly according to the sample topography, is required.

Several FM-AFM methods, such as electrostatic force microscopy and force spectroscopy, are powerful tools for atomic-scale investigations of material properties, therefore applications of these methods to molecular-scale studies of biological functions are strongly expected. In particular, local charge density mapping of biological molecules in a liquid can be a unique method for these studies, since interactions between biological molecules are often based on electrostatic forces. Although high-resolution electrostatic force microscopy (EFM) measurements in UHV have been established, measurements in liquids cannot be conducted easily because of the existence of charged ions, which can be varied depending on the electrostatic potentials of the AFM tip and the sample. The electrically conductive part of the tip must be shielded except for the tip apex, which can be realized by the application of various MEMS techniques as well as advances in liquid AFM technology.

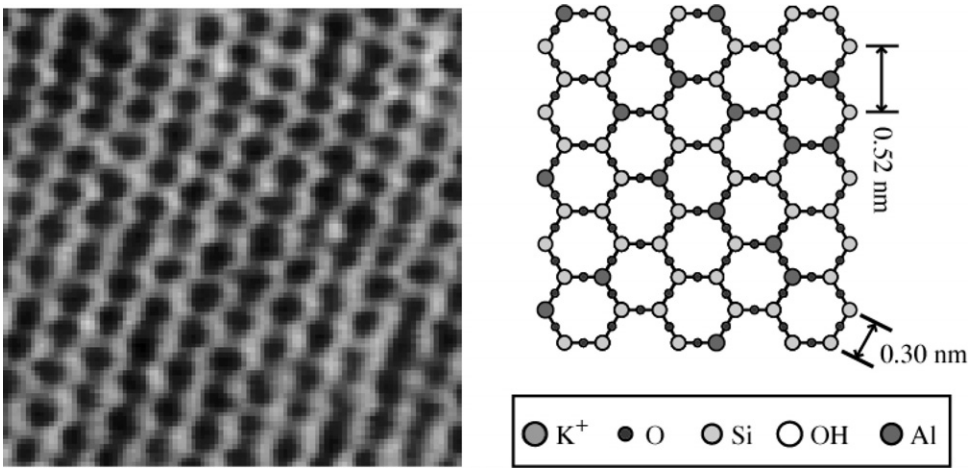

Figure 7. Left: FM-AFM image of the cleaved (001) surface of muscovite mica taken in water. $\Delta f = +200$ Hz, $A = 0.6$ nm. Right: the crystal structure of muscovite mica (cleaved surface).

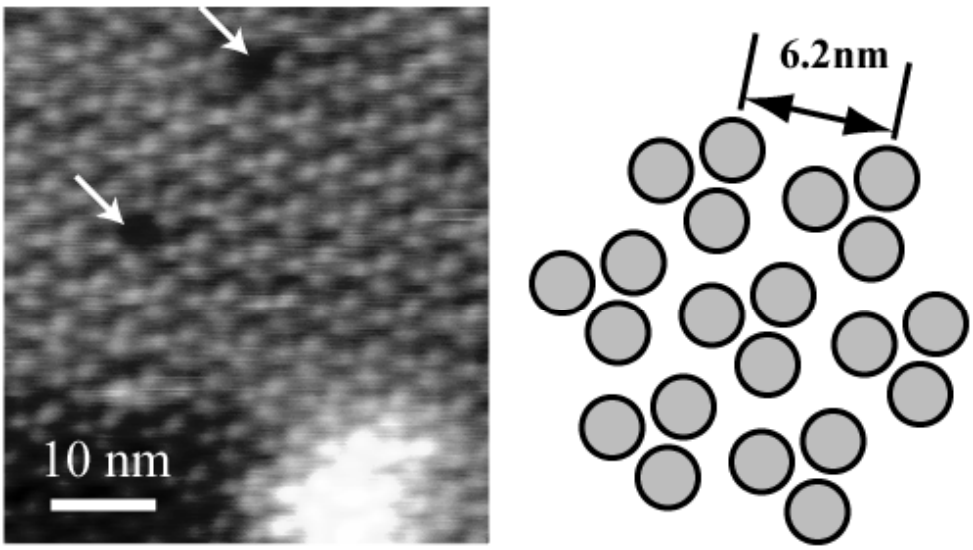

Figure 8. FM-AFM image of a purple membrane on a mica substrate taken in a phosphate buffer solution (10 mM PBS, 50 mM KCl). $\Delta f = +54$ Hz, $A = 1.6$ nm. Right: schematic of hexagonal array structure of bR trimers.

In addition, studies of hydration structures have been carried out by AFM force spectroscopy in liquids [25]. Since the hydration structure measurement strongly depends on the shape and the chemical properties of the AFM tip, the preparation of tips suitable for the solvation/hydration study is crucial. Further developments in the measurement resolution and sensitivity of liquid AFM will possibly expand present AFM studies of hydration structures at a single position into a novel mapping method of three-dimensional hydration structures.

4. High-speed AFM

High-speed AFM has enormous potential. It can be used to visualize moving objects in the nanometre-scale world. In addition, it allows us to assess and/or process a large surface area by scanning its divided areas in rapid succession. Since these innovative abilities will surely create new science and nanotechnology areas, various studies have focused on achieving a high imaging rate.

4.1. Various devices optimized for high-speed scanning

The maximum scan speed is determined by two factors: (1) the maximum frequency at which the scanner can be driven without producing unwanted vibrations; and (2) the bandwidth of feedback operation to maintain the tip–sample interaction force. The scanner has macroscopic dimensions and hence its structural resonant frequency is low. Thus, the scanner is the device that is most difficult to optimize for high-speed scanning. Recent efforts have been successful in overcoming this difficulty. The impulsive forces produced by the quick displacement of piezoactuators are counterbalanced by simultaneous displacement of additional piezoactuators in respective opposite directions [26, 27]. A new technique for actively damping structural and piezoactuator vibrations successfully eliminates their resonant vibrations and at the same time enhances the response speed of piezoactuators [28]. This technique uses a mock scanner (or a mock actuator) whose transfer function is similar to that of the real system.

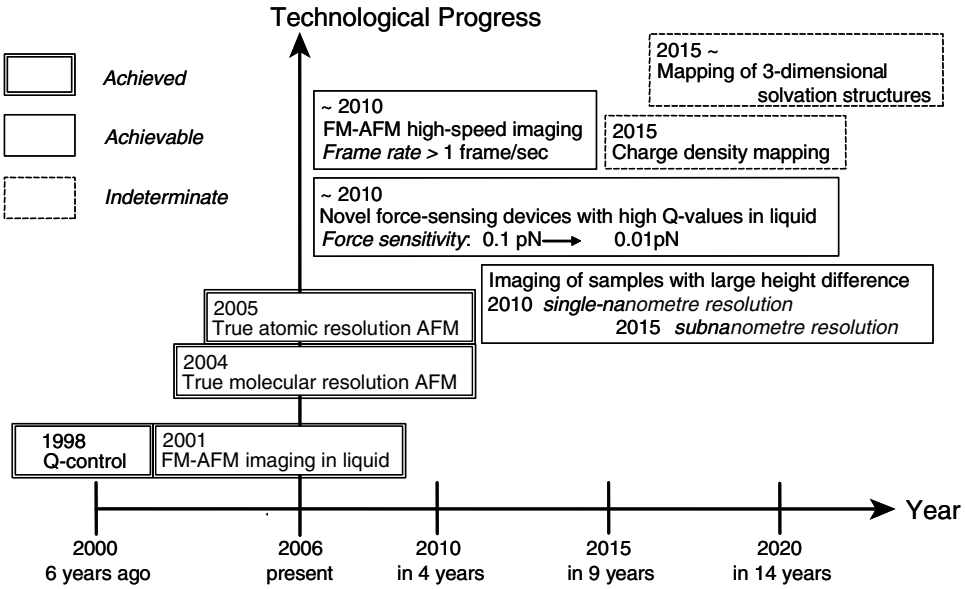

Figure 9. Technology roadmap for FM-AFM imaging in liquid.

However, since the capacity of available piezo-actuators is limited, the bandwidth of the z-scanner is limited to ~150 kHz at present.

The feedback bandwidth is determined by delays that occur in various steps in the feedback loop. In the dynamic mode, a cantilever is oscillated at (or close to) its resonant frequency. Since it takes at least a half cycle of the oscillation to read the amplitude signal even with the fastest detection technique, the feedback bandwidth (defined by the feedback frequency that gives a 45° phase delay) can never exceed 1/4 (in practice ~1/8) of the cantilever's resonant frequency. Therefore, the resonant frequency must be very high, while its spring constant should be kept as small as possible, which requires small cantilevers [29]. Olympus has developed small cantilevers that have resonant frequencies of 3 MHz in air and 1.2 MHz in water, and a spring constant ~0.2 N m^{-1} [30]. The response time of a cantilever is proportional to the quality factor (Q). In water, small cantilevers have Q = 2–3, resulting in a response time of ~0.66 μs. A main delay among others is produced in 'parachuting', which occurs after the cantilever tip completely detaches from the sample surface, especially at a steep downhill region of the sample (i.e. the tip cannot quickly land on the surface again). Complete detachment can be avoided by setting the amplitude set-point deeper, but this setting increases the tip–sample interaction force. The feedback bandwidth quickly decreases with a shallowing setpoint and hence the allowable scan speed depends on the nature of the sample. For hard samples or samples firmly fixed onto the substratum, it is relatively easy to increase the scan speed using a deep setpoint. However, for example, for observations of dynamic interactions of biological macromolecules in a liquid, the tip should barely touch the sample and, accordingly, the setpoint should be very shallow (very close to the cantilever's free oscillation amplitude). Thus, high-speed imaging of the dynamic behavior of fragile samples is quite difficult. A newly developed PID controller (dynamic PID controller) can change its gain parameters automatically, depending on the tip–sample interaction, which eliminates the sharp dependence of the feedback bandwidth on the setpoint [31]. With these devices all together, the feedback bandwidth has reached ~70 kHz. Therefore, protein molecules moving on mica in solution can be captured clearly by video at 60 ms/frame without damaging the sample (see figure 10, left panel). Several movies can be viewed at the following URL: www.s.kanazawa-u.ac.jp/phys/biophys/roadmap.htm.

4.2. Current attempts toward the next generation of high-speed AFM

Various attempts are now underway to enhance the scan speed and to expand the functionality of high-speed AFM. (1) A new method is being developed to enhance the resonant frequency of piezoactuators beyond their natural resonant frequencies without changing the mechanics; the driving signal is manipulated so as to extend the bandwidth of the mechanical transfer function. This is a kind of inverse transfer function compensation and can create an approximate inverse-transfer function for an arbitrary transfer function (figure 11). (2) Direct actuation of a cantilever is usually performed by applying a magnetic field to a cantilever coated with a magnetic material. Because of this coating, the resonant frequency is lowered. Self-actuation cantilevers [32] are the other alternative, but require complicated fabrication processes, which at present results in a relatively low resonant frequency and a large spring constant. Photo-thermal actuation of a cantilever was pioneered by Umeda *et al* [33]. When this technique was applied to our small cantilevers using 405 nm laser light, the dc deflection sensitivity was about 10 nm mW^{-1}. Since no additional coating is required, it does not lower the natural resonant frequency. One drawback is the slow deflection response to changes in the laser power because of slow heat transmission. However, this was successfully eliminated by inverse transfer function compensation [34].

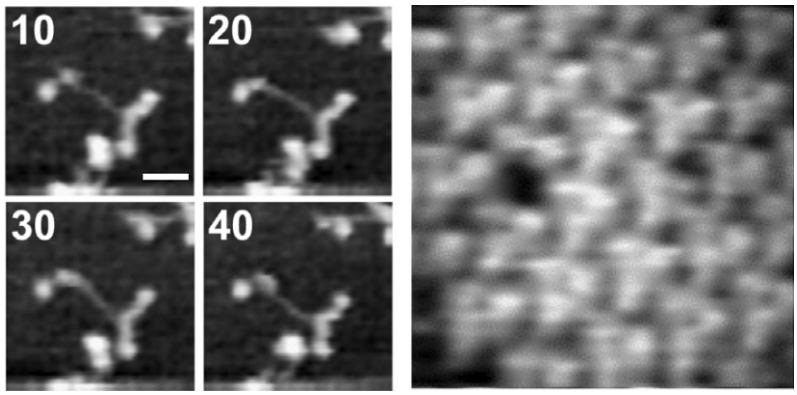

Figure 10. AFM images of myosin V and purple membrane captured by high-speed AFM. Left panel: Clippings of images of myosin V captured at 60 ms/frame for a scan range of 250 nm. The attached numbers are the frame numbers. Scale bar is 37 nm. Right image: Bacteriorhodopsin lattice structure of purple membrane captured by high-speed FM-AFM at 1.9 s/frame. Scan range is 25 nm.

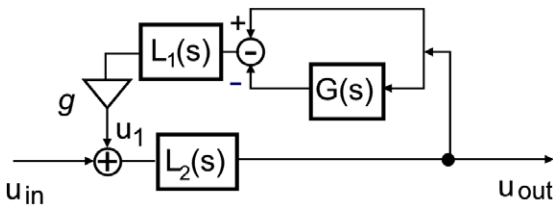

Figure 11. A circuit diagram for producing the inverse transfer function from an arbitrary transfer function. $G(s)$ is a given transfer function, $L_1(s)$ and $L_2(s)$ are low-pass filters representing limited bandwidth of amplifiers used in the circuit, and 'g' is the gain parameter. The transfer function of this circuit becomes $1/G(s)$, when $L_1(s)$, $L_2(s)$ and g are 1. Because of the limited bandwidth of amplifiers used in the circuit, the gain has to be less than 1. To approach $1/G(s)$ more closely, similar circuits can be connected in series with phase compensation by the (1 + differential) operation.

This actuation has great potential to enhance the feedback bandwidth, because the resonant frequency of small cantilevers is much higher than those of available piezoactuators with sufficient displacement. By controlling the tip–sample distance by modulating the laser power, a feedback bandwidth of 100 kHz was recently achieved, which promises video rate imaging for a scan range of ∼150 nm. (3) One of the unique features of dynamic mode AFM is the availability of additional signals for detecting the tip–sample interaction; the phase and resonant frequency of an oscillating cantilever change as a result of the interaction. These signals can afford information on the physico-chemical properties of the sample. Conventional cantilevers need to be oscillated with a large Q for sensitive detection of these signals. In addition, a slow detector, typically a lock-in amplifier, is required to detect small changes in these signals. Therefore, high-speed phase-contrast imaging has been impossible. Since small cantilevers undergo relatively small damping from the surrounding medium, the weak damping that occurs between the tip and the sample is reflected and amplified in the cantilever oscillation. Also, because of the large ratio of the high resonant frequency to the small spring constant, a large shift in the resonant frequency is expected to take place on the tip–sample interaction. A recent attempt with high-speed AM-AFM using small cantilevers (with a small $Q \sim 2$) demonstrated simultaneous in-liquid imaging of topography and phase contrast at ∼70 ms/frame [35]. Even with high-speed FM-AFM, where the Q value of the cantilever was inevitably elevated, relatively fast imaging was demonstrated without using a phase-locked loop (PLL) circuit. A large shift ($> +50$ kHz) in the resonant frequency was observed when the oscillating small-cantilever tip touched the mica surface. As shown in figure 10 (right image), a high-resolution image of the lattice structure formed by bacteriorhodopsin molecules on purple membranes was imaged at 1.9 s/frame.

4.3. Roadmap for high-speed AFM

Figure 12 shows the roadmap for high-speed AFM. The first generation of high-speed AFMs appeared in 2001 [26]. Although moving protein molecules were captured at 80 ms/frame for a scan range of 250 nm, the tip–sample interaction force was too large to image fragile biomolecules without damaging or disturbing their physiological functions. This problem has recently been overcome to some extent by optimizing various devices as mentioned above, which has resulted in successful imaging of protein molecules at work [34, 36]. Video-rate imaging was demonstrated by giving up the electronic feedback operation [37]. Such a high-speed AFM without electronic feedback control can be applied to hard samples with a small height. Video-rate AFM with feedback control will likely be realized soon, probably in one to three years, although the scan size is still limited to ∼250 nm. High-speed AFM with this capacity or somewhat better capacity (∼10 ms/frame) appears to be most useful for studying protein molecules at work, since a protein's functional processes generally take place in this time domain and because dynamic structural changes of protein molecules at work represent the aspect most lacking currently, despite the recent developments of advanced techniques for biological sciences. In ten years, high-speed AFM for biological science will likely be widely distributed in the world, which should activate biological studies and accelerate our understanding of the molecular mechanisms of protein functions.

Thus far, high-speed AFM for industrial applications has not been developed. For industrial uses, the sample stage cannot be scanned; instead, the cantilever has to be scanned

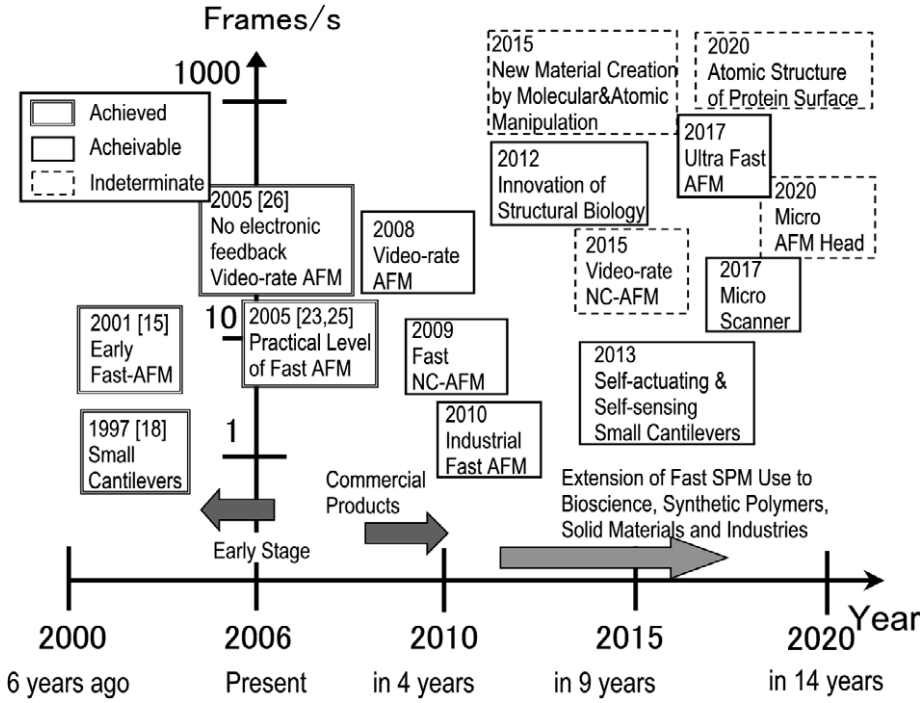

Figure 12. Roadmap 2006 for high-speed AFM. The numbers in square brackets are the reference numbers.

over a large sample surface. In this situation, the system for detecting the cantilever deflection has to be miniaturized to gain high resonant frequency. Self-sensing and self-actuation cantilevers [38] appear to be ideal for such a miniaturized 'cantilever scanner'. This type of cantilever is already available. However, the resonant frequency in air (∼50 kHz) is not sufficiently high. Thus, MEMS technology appears to be key in breaking the present situation to realize innovative high-speed AFMs for industrial uses. Before this innovation, which could occur in 10–15 years, the first version of a high-speed AFM for industrial use will likely appear in five years. Its main target will probably be the semiconductor industry, where high-speed AFMs can play an active role in evaluating semiconductor wafers without damaging them.

Various AFM-related techniques, such as nano-printing and nano-lithography, have been developed for creating nano-structures on surfaces. Also, as mentioned in section 2, the manipulation at room temperature of selected individual atoms with an AFM probe has become possible. The power of these advanced techniques has been demonstrated at the laboratory level. However, at present, the surfaces created cannot be applied for practical use, since the area size of the surfaces created is quite limited because of slow processing and manipulation. Therefore, high-speed AFM will make a great contribution to this field. Newly created surfaces with enough dimensions will become targets to be studied in material science and will also be used by industries that require well-controlled nano-patterns for manufacturing advanced products.

5. Summary

In this paper, recent progress using dynamic mode AFM has been reviewed, focusing on three topics.

(1) Chemical discrimination of intermixed two-atom species and atom-interchange manipulation of heterogeneous two-atom species at RT made by frequency modulation (FM) AFM under ultrahigh vacuum. By converting a precise site-specific frequency shift curve to a site-specific force curve, we have obtained precise short-range force curves of selected single atoms. This method can clarify the chemical covalent force over each species independent of the tip–surface distance. Further, using directional atom interchange, we have constructed embedded atom letters, 'Sn' (the symbol for a tin atom) consisting of 19 Sn atoms embedded in a Ge(111) substrate. Using these methods, we can assemble compound semiconductor nanostructures atom-by-atom.

(2) Submolecular and atomic-resolution imaging even in a liquid by FM-AFM. The use of the small-amplitude mode and large noise reduction in the cantilever deflection sensor has resulted in great progress in FM-AFM imaging in a liquid. Consequently, true atomic-resolution imaging of the cleaved (001) surface of muscovite mica in pure water and submolecular imaging of a purple membrane on a mica substrate in a phosphate buffer solution were demonstrated. Submolecular and atomic-resolution imaging in a liquid is now possible using FM-AFM.

(3) High-speed imaging of biological molecules moving on a substrate in solution by dynamic mode AFM. With several new techniques all together, the feedback bandwidth has reached ∼70 kHz. A recent attempt at high-speed AM-AFM using small cantilevers demonstrated simultaneous in-liquid imaging of topography and phase contrast at ∼70 ms/frame. In addition, a high-resolution image of the lattice structure formed by bacteriorhodopsin molecules on purple membranes was obtained at 1.9 s/frame. High-speed AFM with innovative

abilities is expected to result in the creation of new science and new nanotechnology.

After reviewing the state of the art of these high-performance AFMs and various techniques that have enabled them, the status and future prospects were reviewed from the viewpoint of Japanese groups that have been involved in work in these three topics.

References

[1] Binnig G, Quate C F and Gerber Ch 1986 *Phys. Rev. Lett.* **56** 930
[2] Albrecht T R, Grütter P, Horne D and Rugar D 1991 *J. Appl. Phys.* **69** 668
[3] Giessibl F J 1995 *Science* **267** 68
[4] Morita S, Wiesendanger R and Meyer E (ed) 2002 *Noncontact Atomic Force Microscopy (NanoScience and Technology)* (Berlin: Springer)
[5] Sugimoto Y, Custance O, Jelinek P, Morita S, Pérez R and Abe M 2006 *Phys. Rev.* B **73** 205329
[6] Sugimoto Y, Abe M, Hirayama S, Oyabu N, Custance O and Morita S 2005 *Nat. Mater.* **4** 156
[7] Fukuma T, Ichii T, Kobayashi K, Yamada H and Matsushige K 2005 *Appl. Phys. Lett.* **86** 034103
[8] Ando T, Kodera N, Maruyama D, Takai E, Saito K and Toda A 2002 *Japan. J. Appl. Phys.* **41** 4851
[9] Morita S (ed) 2006 *Roadmap of Scanning Probe Microscopy (NanoScience and Technology)* (Berlin: Springer)
[10] Abe M, Sugimoto Y, Custance O and Morita S 2005 *Appl. Phys. Lett.* **87** 173503
[11] Stipe C, Rezaei M A and Ho W 1998 *Science* **279** 1907
[12] Schwarz A, Allers W, Schwarz U D and Wiesendanger R 1999 *Appl. Surf. Sci.* **140** 293
[13] Foster A S, Barth C, Shluger A L and Reichling M 2001 *Phys. Rev. Lett.* **86** 2373
[14] Bennewitz R, Pfeiffer O, Schär S, Barwich V, Meyer E and Kantorovich L N 2002 *Appl. Surf. Sci.* **188** 232
[15] Okamoto K, Yoshimoto K, Sugawara Y and Morita S 2003 *Appl. Surf. Sci.* **210** 128
[16] Morita S, Sugimoto Y, Oyabu N, Nishi R, Custance O, Sugawara Y and Abe M 2004 *J. Electron Microsc.* **53** 163
[17] Rugar D, Budakian R, Mamin H J and Chui B W 2004 *Nature* **430** 329
[18] Oyabu N, Custance O, Yi I, Sugawara Y and Morita S 2003 *Phys. Rev. Lett.* **90** 176102
[19] Oyabu N, Sugimoto Y, Abe M, Custance O and Morita S 2005 *Nanotechnology* **16** S112
[20] Nishi R, Miyagawa D, Seino Y, Yi I and Morita S 2006 *Nanotechnology* **17** S142
[21] Hirth S, Ostendorf F and Reichling M 2006 *Nanotechnology* **17** S148
[22] Fukuma T, Kobayashi K, Matsushige M and Yamada H 2005 *Appl. Phys. Lett.* **86** 193108
[23] Hoogenboom B W *et al* 2005 *Appl. Phys. Lett* **86** 074101
[24] Fukuma T, Kimura M, Kobayashi K, Matsushige K and Yamada H 2005 *Rev. Sci. Instrum.* **76** 053704
[25] Jarvis S P, Uchihashi T, Ishida T, Tokumoto H and Nakayama Y 2000 *J. Phys. Chem.* B **104** 6091
[26] Ando T, Kodera N, Takai N, Maruyama D, Saito K and Toda A 2001 A high-speed atomic force microscope for studying biological macromolecules *Proc. Natl Acad. Sci. USA* **98** 12468
[27] Fantner G E *et al* 2006 Components for high speed atomic force microscopy *Ultramicroscopy* **106** 881
[28] Kodera N, Yamashita H and Ando T 2005 Active damping of the scanner for high-speed atomic force microscopy *Rev. Sci. Instrum.* **76** 053708
[29] Schäffer T E, Viani M, Walters D A, Drake B, Runge E K, Cleveland J P, Wendman M A and Hansma P K 1997 An atomic force microscope for small cantilevers *Proc. SPIE* **3009** 48
[30] Kitazawa M, Shiotani K and Toda A 2003 Batch fabrication of sharpened silicon nitride tips *Japan. J. Appl. Phys.* **42** 4844
[31] Kodera N, Sakashita M and Ando T 2006 A dynamic PID controller for high-speed atomic force microscopy *Rev. Sci. Instrum.* **77** 083704
[32] Itoh T, Lee C and Suga T 1996 Deflection detection and feedback actuation using a self-excited piezoelectric $Pb(Zr,Ti)O_3$ microcantilever for dynamic scanning force microscopy *Appl. Phys. Lett.* **69** 2036
[33] Umeda N, Ishizaki S and Uwai H 1991 Scanning attractive force microscope using photothermal vibration *J. Vac. Sci. Technol.* B **9** 1318
[34] Ando T, Uchihashi T, Kodera N, Miyagi A, Nakakita R, Yamashita H and Sakashita M 2005 High-speed atomic force microscopy for studying the dynamic behavior of protein molecules at work *Japan. J. Appl. Phys.* **45** 1897
[35] Uchihashi T, Yamashita H and Ando T 2006 Fast phase imaging in liquids using a rapid scan atomic force microscope *Appl. Phys. Lett.* **89** at press
[36] Ando T, Kodera N, Uchihashi T, Miyagi A, Nakakita R, Yamashita H and Matada K 2005 High-speed atomic force microscopy for capturing dynamic behavior of protein molecules at work *e-J. Surf. Sci. Nanotech.* **3** 384
[37] Humphris A D L, Miles M J and Hobbs J K 2005 A mechanical microscope: High-speed atomic force microscopy *Appl. Phys. Lett.* **86** 034106
[38] Manalis S R, Minne S C and Quate C F 1996 Atomic force microscopy for high speed imaging using cantilevers with an integrated actuator and sensor *Appl. Phys. Lett.* **68** 871